

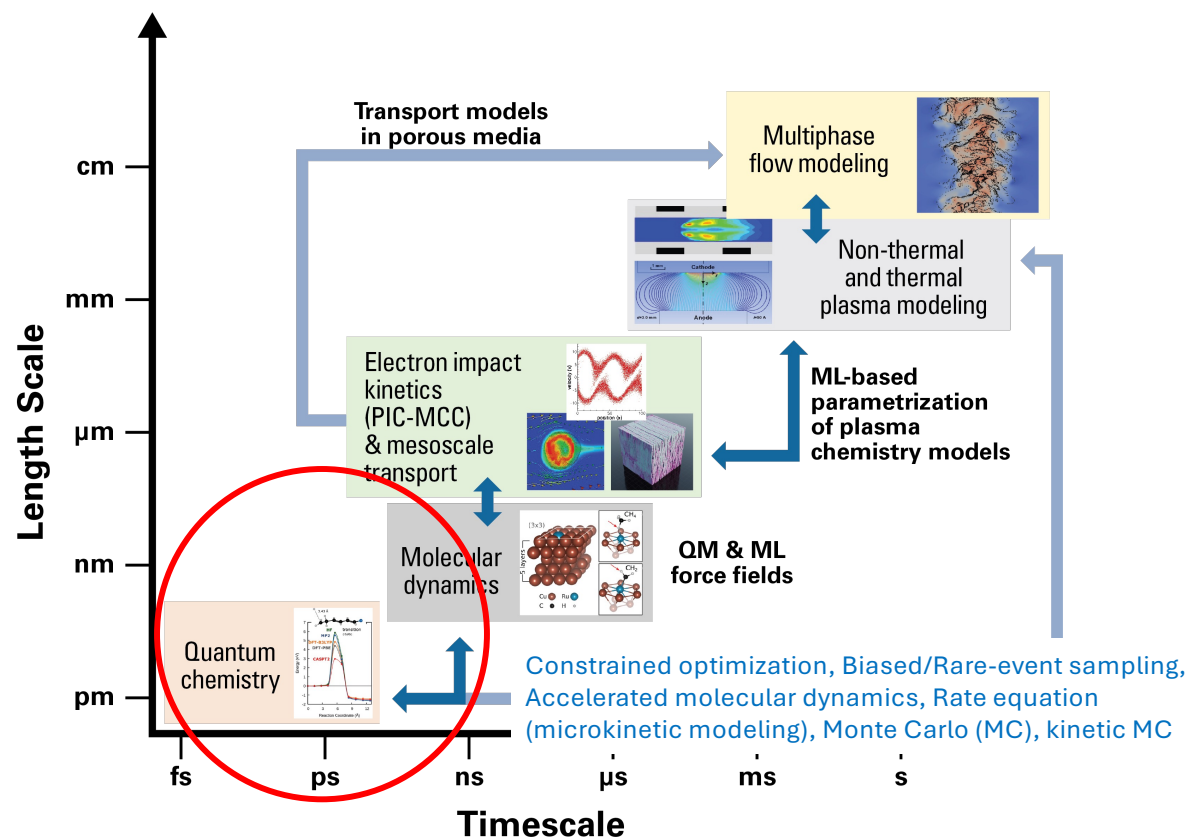
Modeling excited-state chemistry and quantum defects via quantum mechanics

John Mark P. Martirez

Applied Materials and Sustainability Sciences
Princeton Plasma Physics Laboratory
Princeton University

July 30, 2025

Temporal and spatial scales of reactions and enabling computational methods



Multi-level and multi-scale schemes can facilitate systematic understanding of the elementary processes, from atomic-scale chemistry to continuum physics

Continuum physics-based models for millisecond and micrometer-scale phenomena (longer/larger)

DFT for short MD simulations

DFT-based ML force-fields enable proper sampling of slow/rare events (or even parameterization of continuum models)

Correlated wavefunction theory and Density functional theory (DFT) for elementary chemical reactions in gas/plasma and surfaces

Hierarchy of Quantum mechanical (QM) methods

Solve Schrodinger Equation:

$$H\psi(r, R) = E\psi(r, R)$$

Approximations introduced - mostly physically guided/inspired

Ideally, **errors are tractable**, and method is **systematically improvable** (fortuitous error cancelation occurs)

Not all methods are created equal

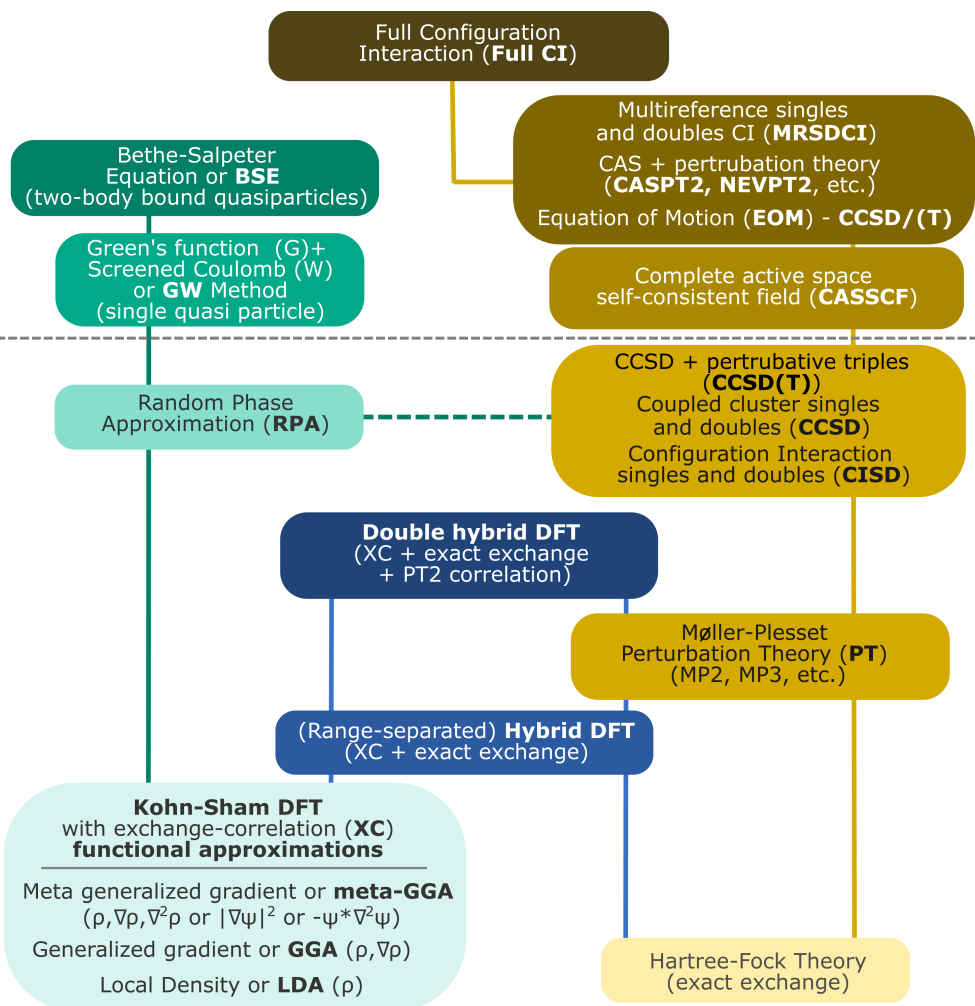
Electron and nuclear degrees of freedom separated (Born-Oppenheimer – “fixed” nuclei); nuclei generally treated classically

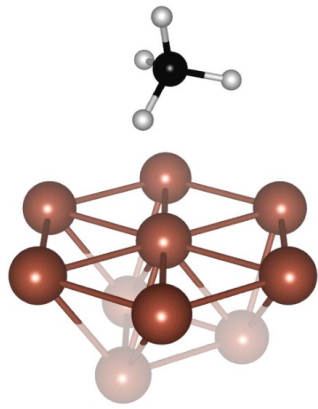
In QM, one starts with classical interactions of electrons and nuclei (Coulomb – charged particles) and electrons’ kinetic energy (a wave)

Systematically add quantum “world” effects – electron exchange (Pauli exclusion principle) and correlation (correlated electron motion reducing Coulomb repulsion, electron as wave)

Chemical accuracy ~ 0.043 eV $\rightarrow r \propto \exp(\pm E/k_B T)$
 ~ 6 or $1/6$; DFT errors $\sim 0.1 - 1.0$ eV

Ground & Rigorous Excited State Theories

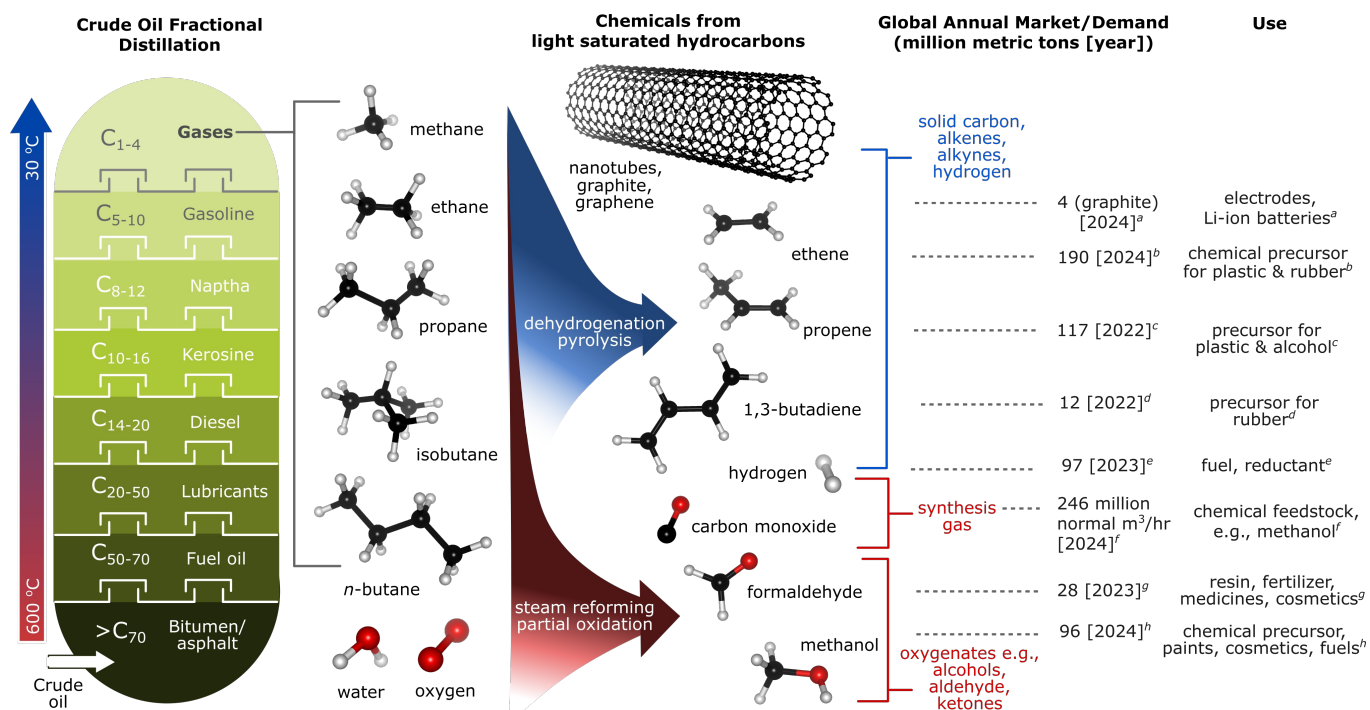




Excited-State Chemistry

Enabled by Light and Plasma

Chemical production and manufacturing

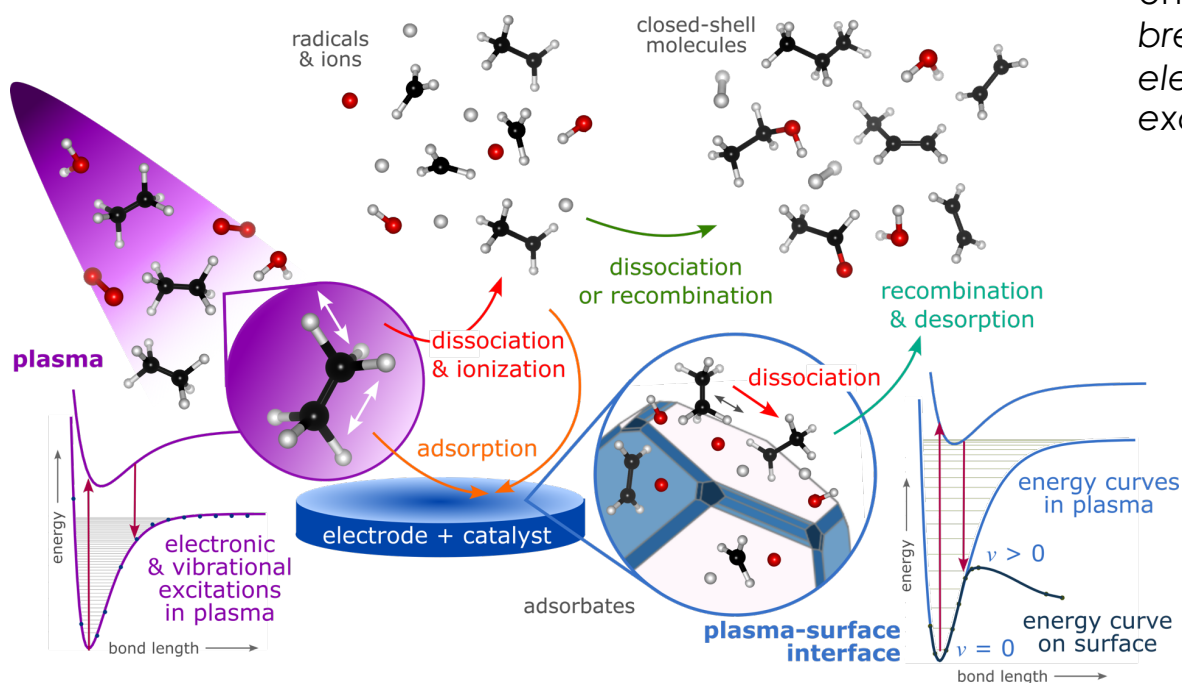


Light gases from petroleum are important chemical feedstocks to generate chemical precursors → produce economically important commodities, e.g., plastic, rubber, alcohols, fertilizers, cosmetics, etc.

Their conversion are typically facilitated by heat (fossil fuel combustion)

How can we enable electrification and decentralization? **Plasma?**

Chemical processes in (low-temperature) plasma (and photolysis)



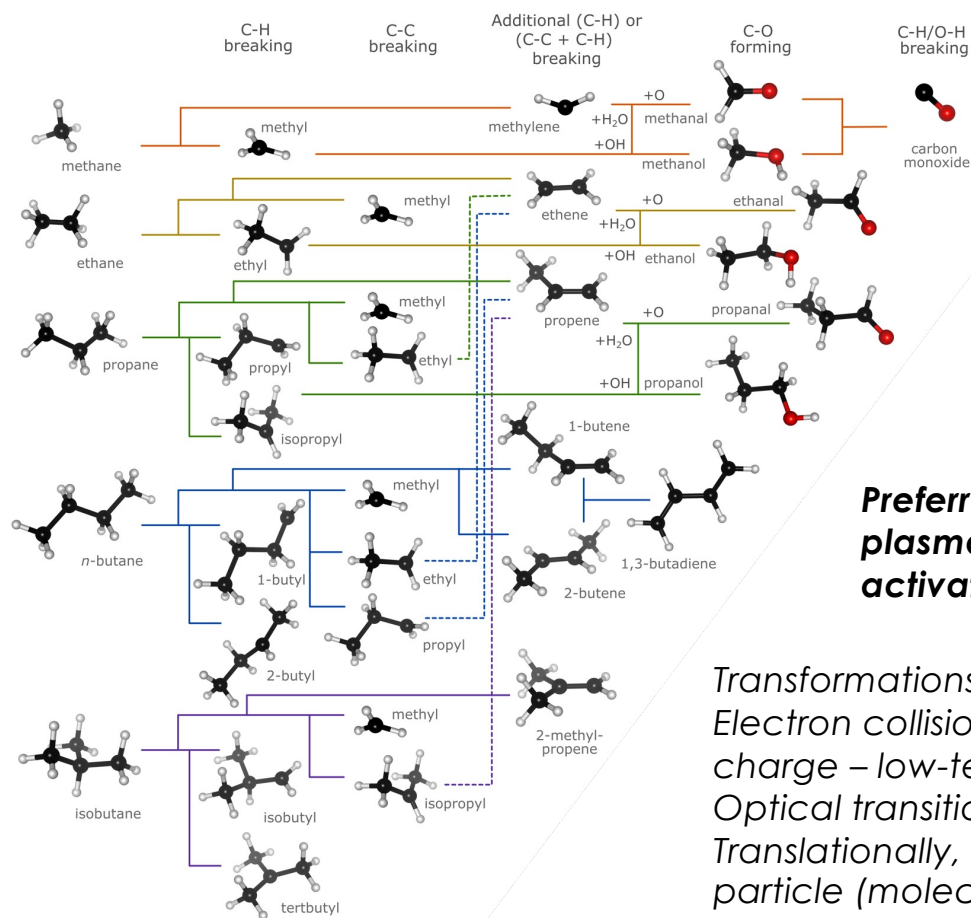
Energy dissipation channels of molecules after collision with an energetic electron (e^-) in plasmas: *break/form bonds; lose/gain electron(s); electronically/vibronically excited*

Surfaces may influence preferred channel:
chemistry-driven

Explore role of heterogenous catalysts e.g., *Cu and Pt* in plasma-assisted partial dehydrogenation of light alkanes

Excited-state methods for molecules are essential

Dehydrogenation and partial oxidation of light hydrocarbons



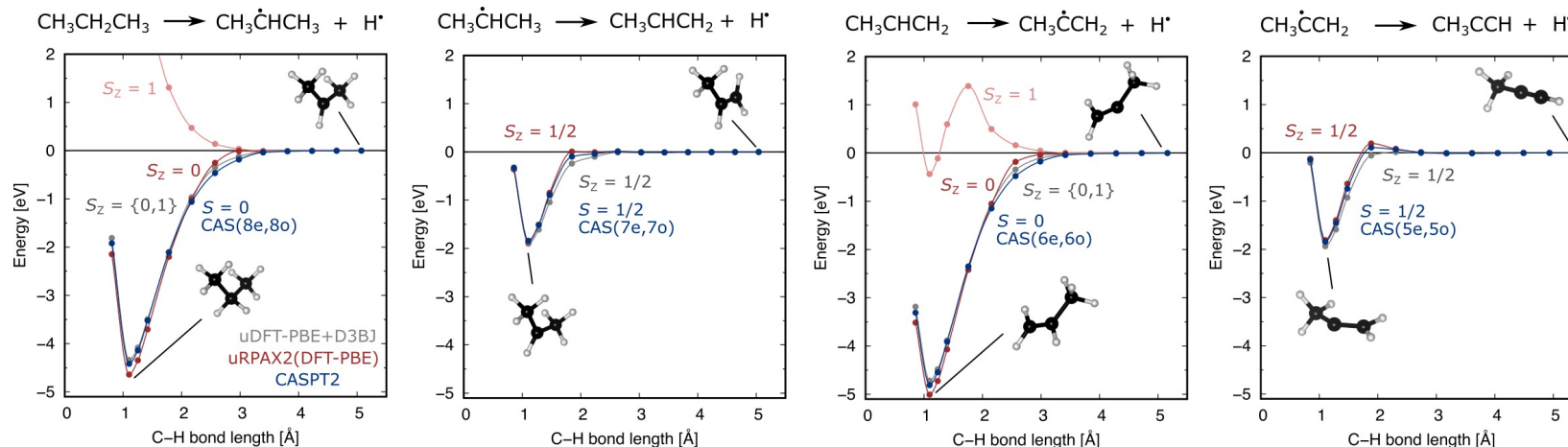
Chemistry may be (beautifully) complex but can be tractable

Dissociation channels are primary routes (C-H and C-C - easier), but **new bonds may also form** (C-C, C-O, O-H)

Preferred processes may be **different** between **plasma**, **photolysis** (light-driven) and **thermal activation** (heat-driven)

Transformations are driven by:
 Electron collisions, imparting energy and sometimes charge – low-temperature plasmas;
 Optical transition – photolysis;
 Translationally, rotationally, & vibrationally energized particle (molecules and atoms) collisions – thermal;

Comparing QM methods: propane dehydrogenation gas-phase energetics



Reaction \ Reaction Energy (eV)	$\Delta(H_f(0K)-ZPE)_{exp}$	uDFT-PBE+D3BJ	uRPAX2	CASPT2	NEVPT2
$CH_3CH_2CH_3 \rightarrow CH_3HC=CH_2 + H_2$	1.60	1.70	1.71	1.65	1.50
$CH_3HC=CH_2 \rightarrow CH_3C\equiv CH + H_2$	1.99	2.12	2.02	2.05	2.02

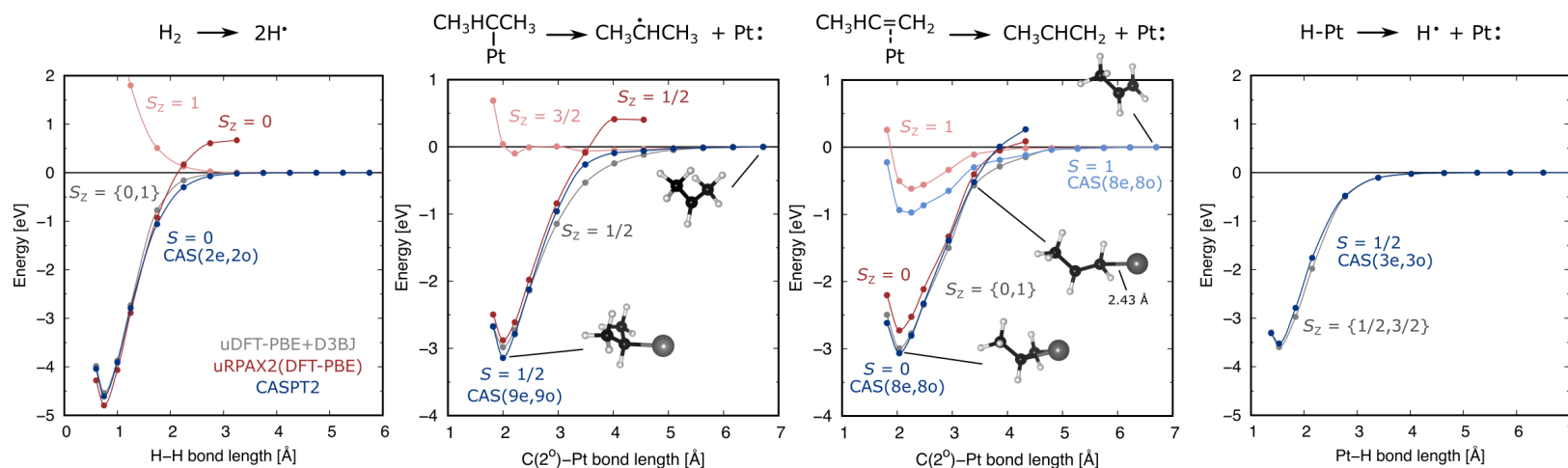
Accurate predictions across the board: spin-unrestricted (spin-contaminated) DFT-PBE+D3BJ and RPA(DFT-PBE) vs. spin-restricted multireference CASPT2/NEVPT2

exp : Computational Chemistry Comparison and Benchmark Database NIST (<https://cccbdb.nist.gov>)

Unrestricted DFT-PBE+D3BJ
C,H – PAW, planewave, 700 eV kinetic energy cut-off

RPAX2 : A. Heßelmann, *Phys. Rev. A*, 85, 012517 (2012)
CASPT2 : H.-J. Werner, *Mol. Phys.* 89, 645 (1996)
NEVPT2 : C. Angeli, et al., *J. Chem. Phys.*, 114,10252, (2001)
C,H – All-electron; aug-cc-PVTZ

Comparing QM methods: H-H and Pt-C/Pt-H bond dissociation



Reaction \ Reaction Energy (eV)	$\Delta(H_f(0K)-ZPE)_{exp}$	uDFT-PBE+D3BJ	uRPAX2	CASPT2	NEVPT2
$H_2 \rightarrow 2H$	4.75	4.54	4.79	4.61	4.53
$CH_3CH_2CH_3 \rightarrow CH_3CH=CH_2 + H_2$	1.60	1.70	1.71	1.65	1.50
$CH_3HC=CH_2 \rightarrow CH_3C\equiv CH + H_2$	1.99	2.12	2.02	2.05	2.02

exp : G. Herzberg, A. Monfils, J. Mol. Spectrosc. 5, 482 (1961); <https://cccbdb.nist.gov>

Unrestricted DFT-PBE+D3BJ
C,H,Pt – PAW, planewave,
700 eV kinetic energy cut-off

RPAX2 : A. Heßelmann, Phys. Rev. A, 85, 012517 (2012)

CASPT2 : H.-J. Werner, Mol. Phys. 89, 645 (1996)

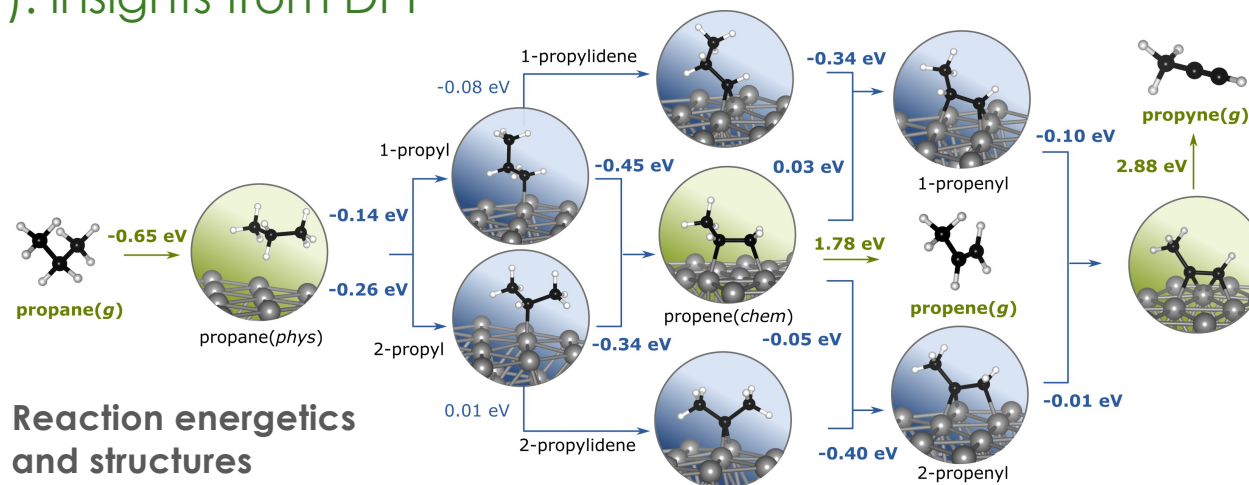
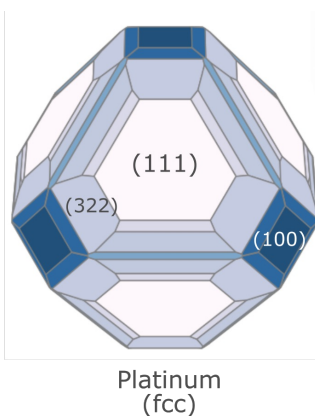
NEVPT2 : C. Angeli, et al., J. Chem. Phys., 114, 10252, (2001)
C,H – All-electron; aug-cc-PVTZ,
Pt – 80-electron ECP; aug-cc-PVTZ

Spin-unrestricted DFT-PBE+D3BJ
comparable to CASPT2

Spin-unrestricted RPAX2(DFT-PBE) : the same as DFT-PBE+D3BJ for H_2 , **but under-binds Pt- C_3H_x complexes and fails convergence for Pt-H**

Propane dehydrogenation mechanism on Pt(111): insights from DFT

Stable surfaces of face-centered cubic platinum (Pt) Wulff construction – shape that minimizes the surface energy (equilibrium) given a crystal volume



Reaction energetics and structures

Periodic DFT-PBE+D3BJ

(atomic models: C, H, Pt – black, white, grey spheres)

C, H, Pt – PAW potentials
Planewave 660 eV kinetic energy cut-off
Five-layer (3 x 3) Pt(111) slab, 7x7x1 k-point mesh

- ✓ Dehydrogenation at the 2° carbon preferred
- ✓ Decomposition energetically down hill on Pt(111)
- ✓ Strong Pt-H bond (desorption energy of H₂ = 1.09 eV/H₂)
- ✓ 1- or 2-propenyl formation favored over propene desorption

X propene and propyne too strongly bound

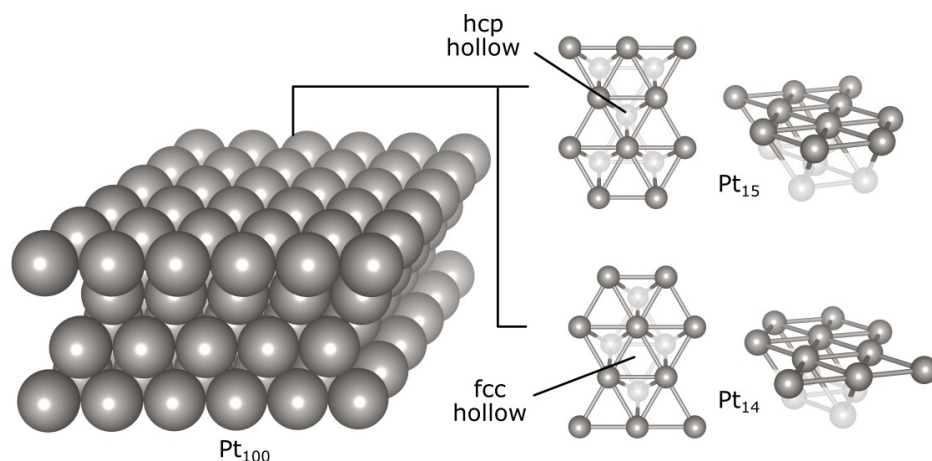
How reliable are the calculated energetics?

Divide and Conquer: Combining DFT and correlated wavefunction methods for surface reactions

Density Functional Embedding Theory (DFET)

Embedding scheme:

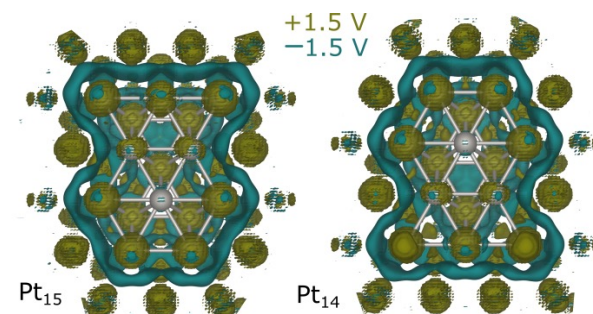
Density functional embedding theory +
Embedded correlated wavefunction (CW) theory



$$\max \left[W = E_{eDFT}^A[\rho^A, V_{emb}] + E_{eDFT}^B[\rho^B, V_{emb}] - \left\{ \int V_{emb} \rho^{A+B} dr \right\} \right]$$

$$\frac{\delta W}{\delta V_{emb}(\mathbf{r})} = \frac{\delta E_{eDFT}^A}{\delta V_{emb}(\mathbf{r})} + \frac{\delta E_{eDFT}^B}{\delta V_{emb}(\mathbf{r})} - \frac{\delta E_{DFT}^{A+B}}{\delta V_{emb}(\mathbf{r})}$$

$$\approx \rho^A[V_{emb}](\mathbf{r}) + \rho^B[V_{emb}](\mathbf{r}) - \rho^{A+B}(\mathbf{r})$$

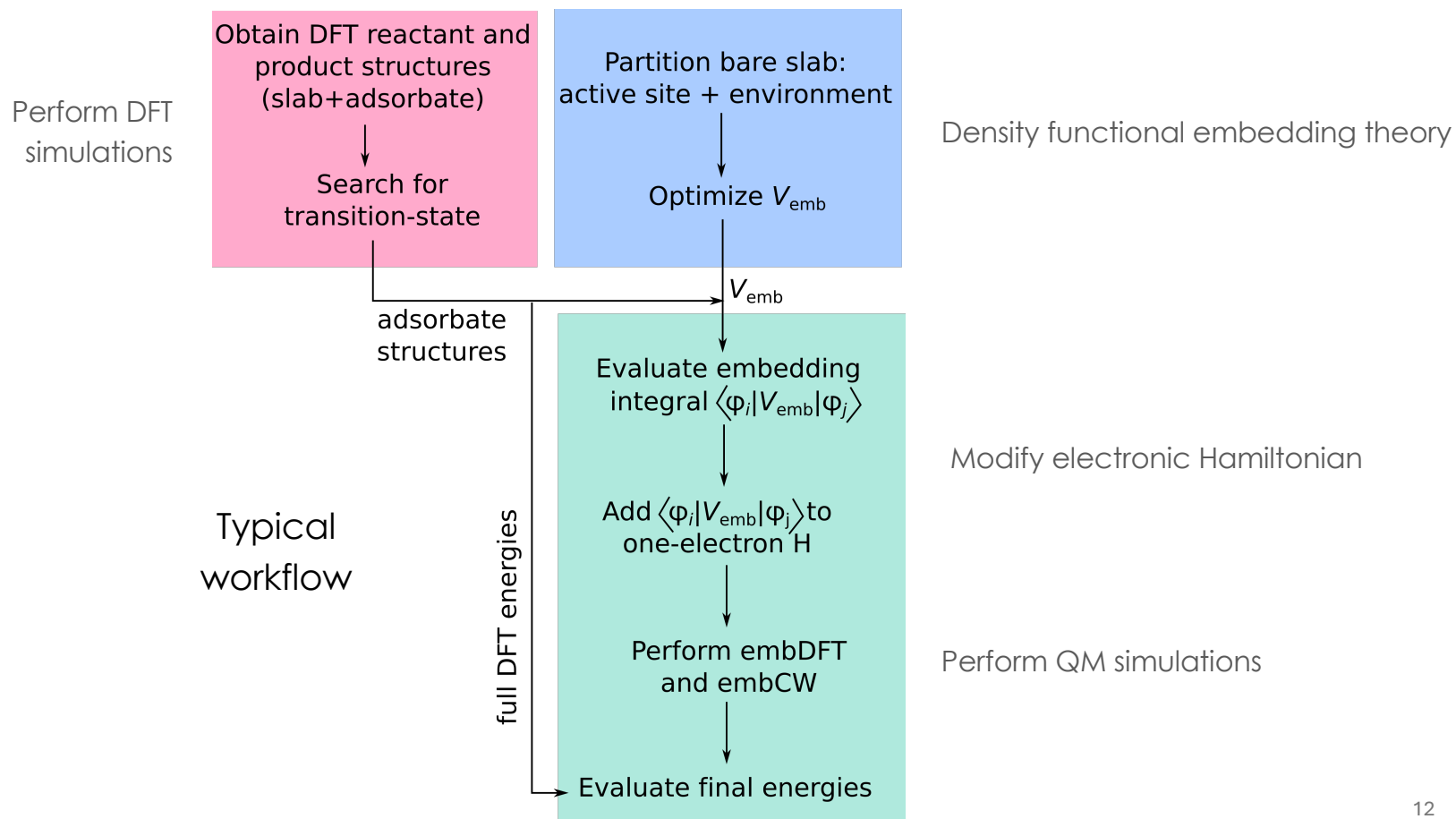


$$E^{DFET} = E_{full}^{PW-DFT} + (E_{cluster}^{embGTO-CW}[V_{emb}] - E_{cluster}^{embGTO-DFT}[V_{emb}])$$

Refinement for ground-state reaction
energy surfaces AND enables **accurate**
treatment of excited-state surfaces

C. Huang, M. Pavone, E. A. Carter, *J. Chem. Phys.*, 134, 154110 (2011)
K. Yu, F. Libisch, E. A. Carter, *J. Chem. Phys.*, 143, 102806 (2015)

Divide-and-Conquer: DFET and embedded CW workflow



Select Pt(111) surface reaction energetics from ECW theory

**DFT(PBE)+D3BJ
vs. emb-
CASPT2/NEVPT2**
(w/ experimental
benchmarks)

Experimental values

(0K- extrapolated and ZPE removed)

Propane on Pt(111): M.C. McMaster, et al.,
Chem. Phys., 177, 461 (1993)

H on Pt(111): B. Poelsema, et al., *J. Phys.*
Condens. Matter, 22, 304006 (2010)

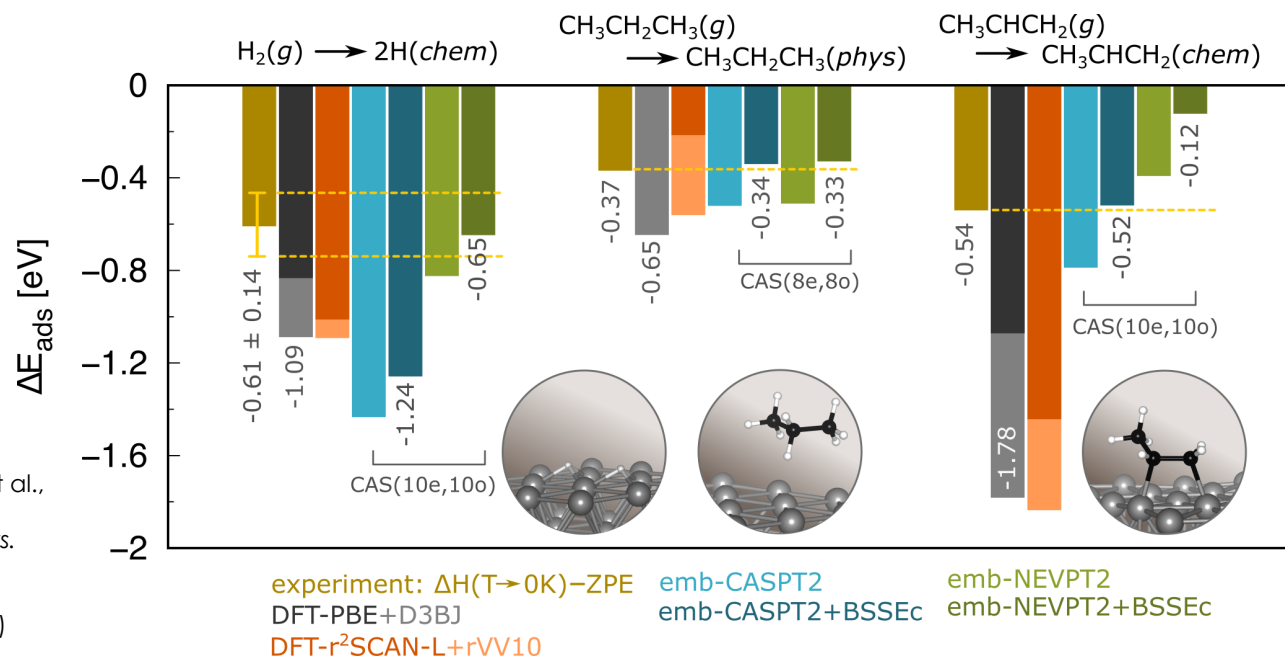
Propene on Pt(111): M. Salmeron, G.A.
Somorjai, *J. Phys. Chem.*, 86, 341 (1982)

Restricted DFT-PBE+D3BJ

C,H,Pt – PAW, planewave, 660 eV
kinetic energy cut-off

CASPT2 and NEVPT2

C,H – All-electron; aug-cc-PVTZ
Pt – 80-electron ECP; aug-cc-PVTZ

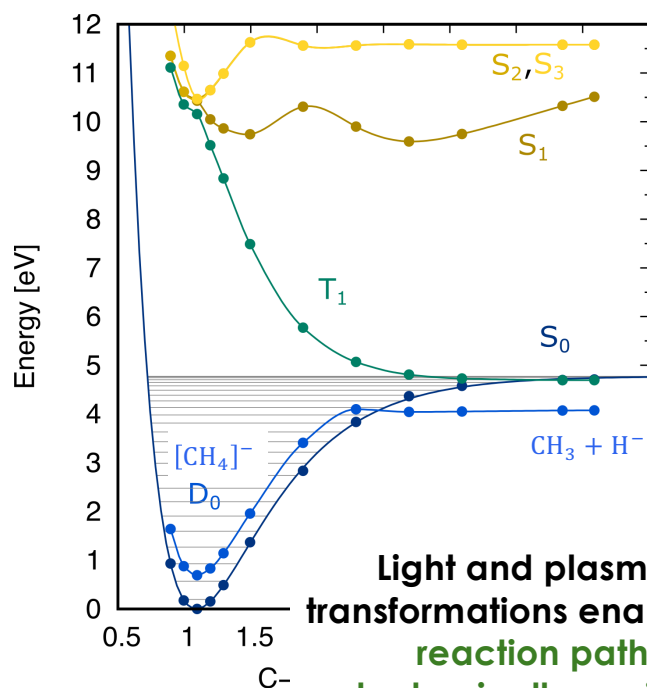


- DFTs and embCASPT2 over-bind *H on Pt(111)
- embNEVPT2 ($\theta_H = 0.222$ H coverage, $2H^*$ adjacent fcc sites) within experimental range ($\theta_H = 0.1$ to 1.0)
- **Improvement in prediction accuracy across the board when using correlated wavefunction methods**

Excited-state decomposition of gaseous methane

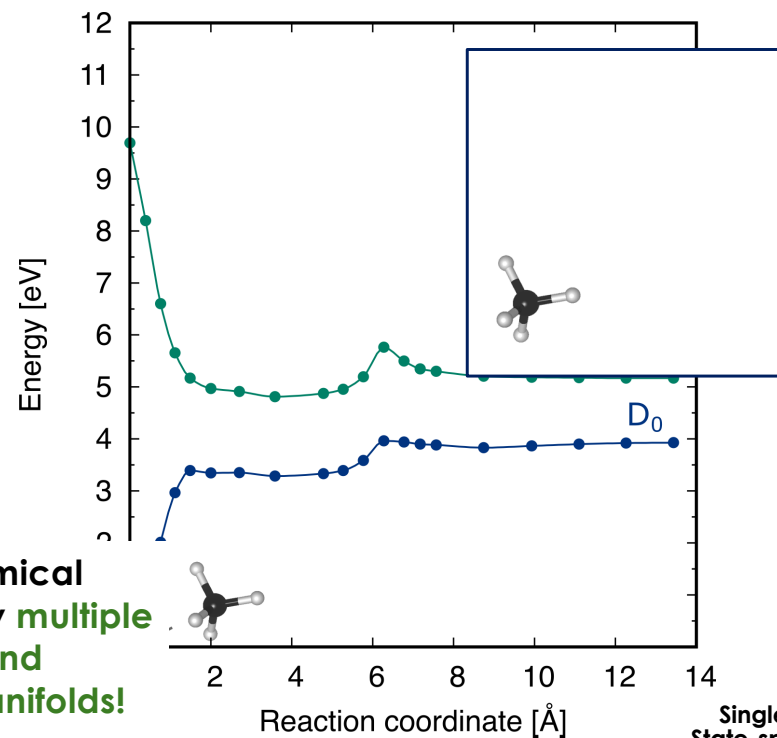
vertical excitation energy (V_{ee}) = 10.4 eV
 vertical ionization energy = 14.2 eV (exp = 13.6 eV)
 vertical electron affinity (V_{EA}) = -0.72 eV

Dissociative electron impact excitation



Light and plasma: chemical transformations enabled by multiple reaction pathways and electronically excited manifolds!

Dissociative electron attachment

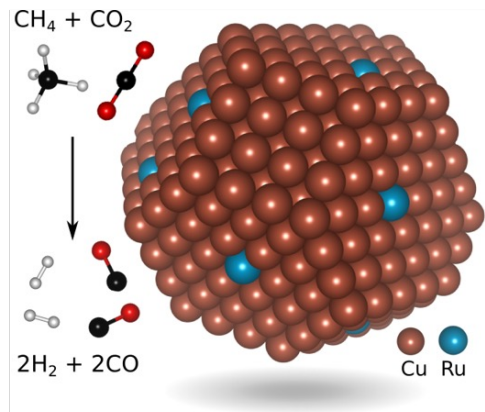


Single-state CASPT2
 State-specific CASSCF
 active space: (9e,9o), basis set: aug-cc-pvtz
 DFT structures

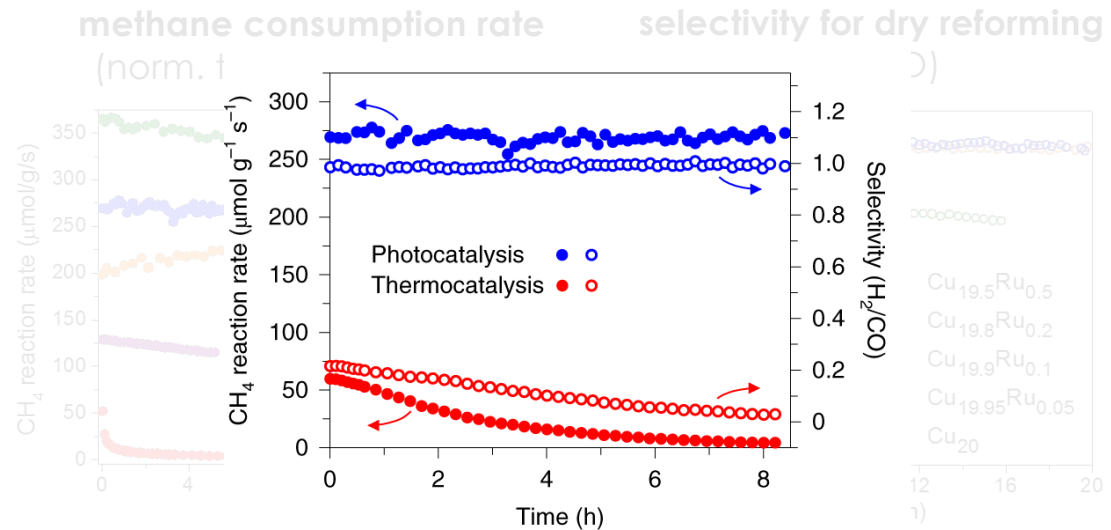
(Four-state) multi-state CASPT2
 State-averaged CASSCF
 active space: (8e,8o), basis set: aug-cc-pvtz
 DFT structures

Light-activated (plasmonic) catalysis: methane dry reforming to syngas (industrially important chemical precursor)

Methane dry reforming on Ru-doped Cu



- H₂ + CO (syngas)
- Cu nanoparticles <10 nm (varying low Ru fractions) on MgO/Al₂O₃
- white light illumination (19.2 W-cm⁻², room temp.)



Conversion of thermal vs. photo (Cu:Ru = 100:1)

- Higher Ru content leads to higher activity
- Low Ru subject to deactivation

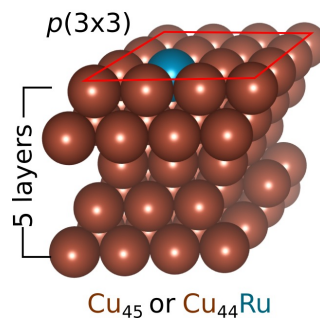
Effective (light) and thermocatalytic (dark) temperatures ~ 1000 K.

Light = 19.2 W/cm² white light

selectivity increases with Ru content BUT decreases at high a content (competing reaction)

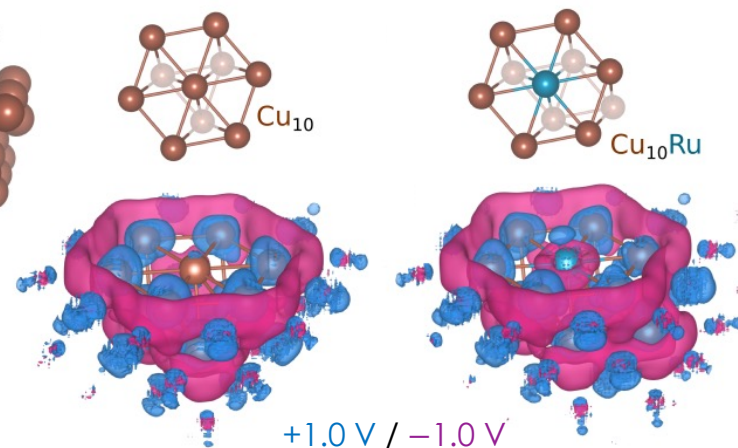
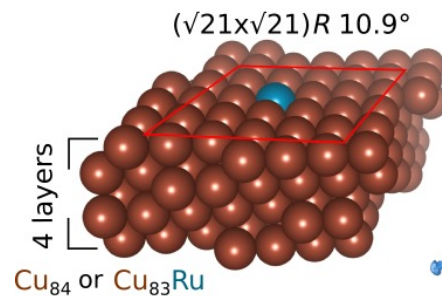
Slab and cluster models

C-H bond breaking
(forming CH₃, CH₂, CH,
and C fragments) **slow**



Periodic DFT (PBE+D3BJ) with
semiempirical van der Waals
correction for *reaction*
pathways

Embedding
potential from **DFET**

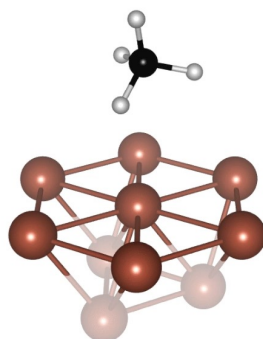


Excited-state C-H bond activation from embedded NEVPT2

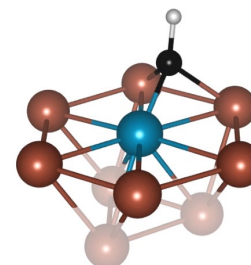
First C-H bond breaking
most difficult on **pure Cu**

Fourth C-H bond
breaking for **Ru** single
atom on **Cu**

NEVPT2 using
multiconfigurational
CASSCF with an
active space of
(10e,10o) as
reference



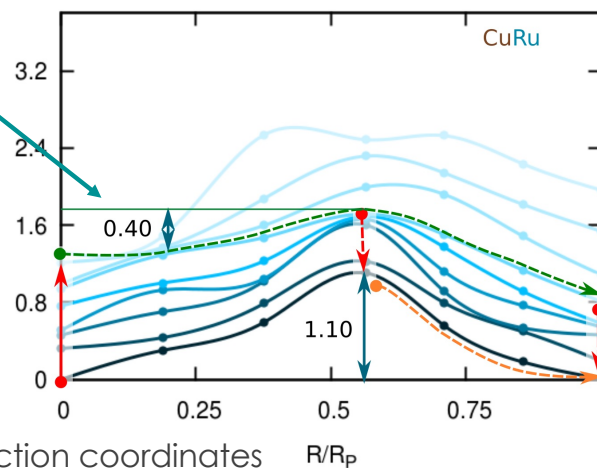
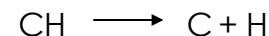
Key:
Cu/Ru/C/H



Relative Energy [eV]

Moderate ground-state barrier,
an **excitation energy of ~1.4 eV**
enough to almost
overcome the barrier

visible light activated!
(barrier from 1.1 eV to 0.4 eV)



CASSCF : H.-J. Werner, *Mol. Phys.* 89, 645 (1996)

NEVPT2 : C. Angeli, et al., *J. Chem. Phys.*, 114,10252, (2001)

L. Zhou, et al.; **Nat. Energy**, 5, 61 (2020)

R/R_p reduced reaction coordinates R/R_p

Summary

Spin-contaminated DFT with semi-local (PBE) exchange-correlation functional proved to be **adequate for gas-phase hydrocarbon dehydrogenation** chemistry

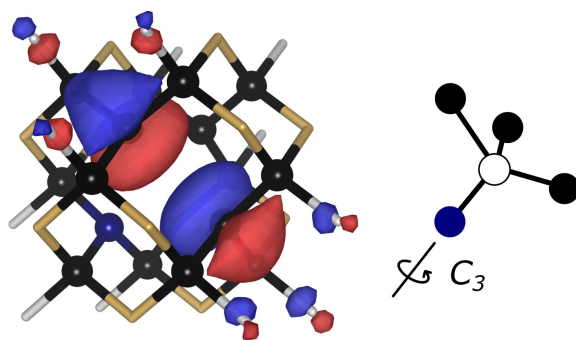
Spin-unrestricted RPA show similar performance as DFT for gas-phase rxns., although **worse for an open shell transition metal atom (Pt)**

Newer generation XC functional r²SCAN-L with rVV10 vdW correction predicts similarly as PBE + D3BJ for H₂ and C₃H_x adsorption on Pt(111) – does not justify increase computational cost

Multireference perturbation theories (enabled by DFET for surfaces) produce the best result across the board – gaseous and surface reactions

Multireference perturbation theories provide **valuable insight** into **excited-state chemical processes**

Surfaces may influence conversion pathways for excited state species harnessed through plasma or light excitations

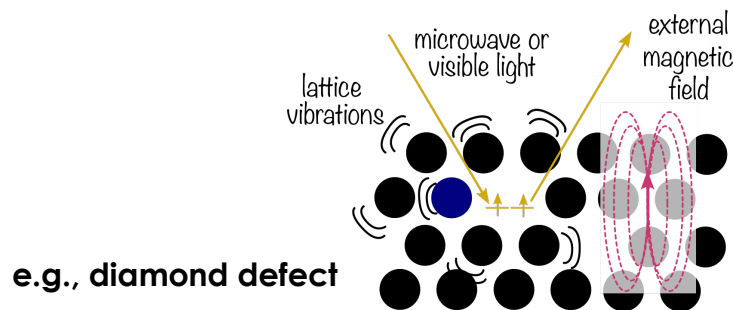


Using **Quantum Mechanics**
For Designing **Qubits**

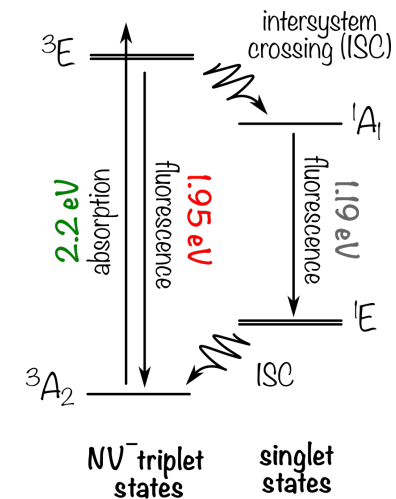
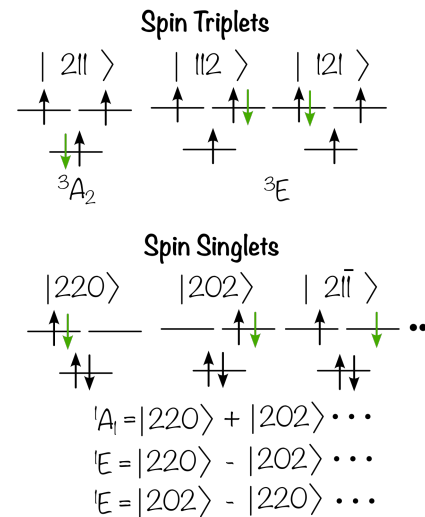
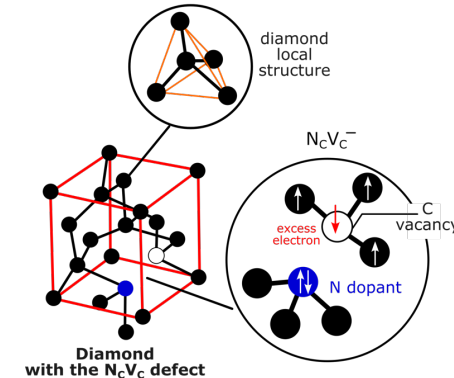
Optical and magnetic properties of diamond "color centers"

Qubits (quantum bits)

- **Basic units of information** in quantum devices that **enable computation, communication, and sensing**
- Takes advantage of **quantum phenomena: electron and nuclear spins, state superposition, & entanglement**
- **Prepared/manipulated via static magnetic field** (energy splitting **via Zeeman effect**); generate a coherent state (different m_s sublevels) via microwave (zero-field splitting energy)
- **Pumped using visible light excitation**
- **Probed measuring emission (fluorescence)**



Example: negatively charged NV center in diamond

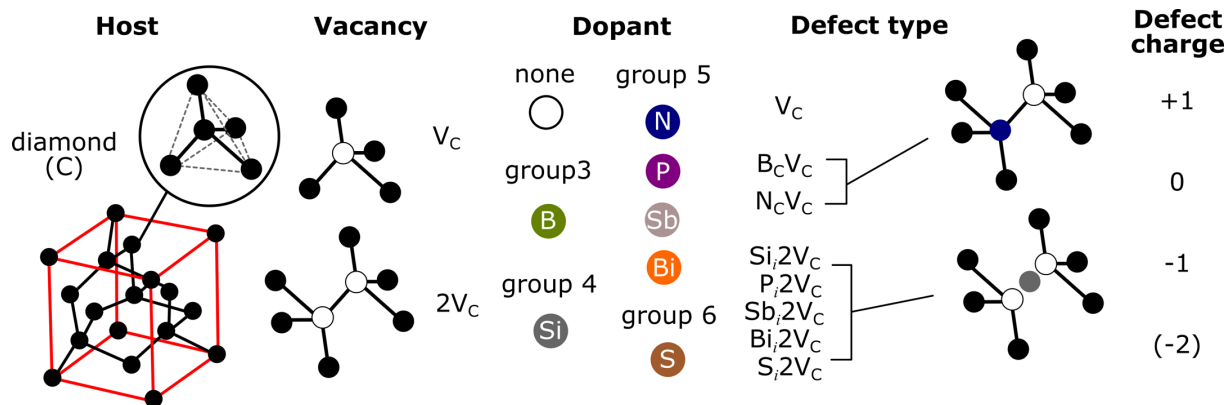


Exploring novel “quantum” defects in diamond

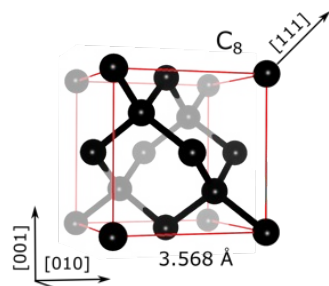
Diamond

- **Wide-band gap** (5.5 eV) group IV semiconductor
 - **Diamagnetic** (“nonmagnetic”)
 - Can form **magnetic defects**
 - High breakdown voltage
 - Can be made with **high purity and precisely placed defects**

Ferrenti, A. M., de Leon, N. P., Thompson, J. D. & Cava, R. J., *npj Computational Materials* 6, 126 (2020)



QM method benchmarking for pure diamond



Band gap of pure diamond: Different DFT exchange correlation functionals and quasi-particle method vs. experiment

Table 1. Predicted lattice constant and indirect band gap^a for a pristine diamond (C₈ supercell) from different DFT approximations compared to the experimental structure and fundamental band gap.

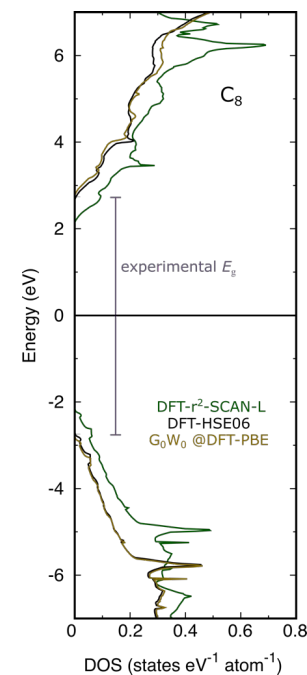
Method	Cubic a (Å)	E_g (eV)
Experiment	3.56712 ± 0.00005^b	5.480 ± 0.004^c
DFT-r ² -SCAN-L	3.5677	4.22 ± 0.02
DFT-HSE06	-	5.30 ± 0.02
G ₀ W ₀ @DFT-PBE	-	5.50 ± 0.02^d

^aDifference between the energies of the **conduction band minimum**
and valence band maximum

^bX-ray diffraction at room temperature, Yamanaka, T. & Morimoto, S.
Acta Crystallographica Section B 52, 232 (1996)

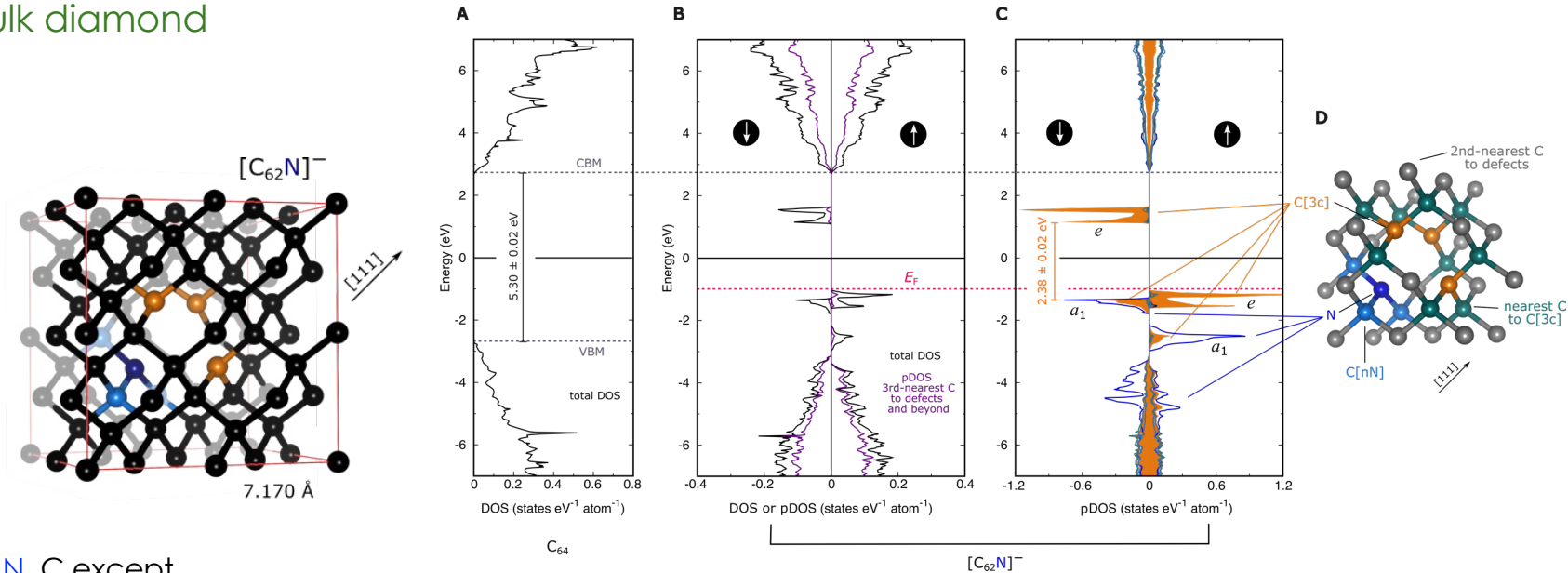
^cphotoemission-inverse photoemission, Cheng, L., Zhu, S., Ouyang, X. &
Zheng, W., Diamond and Related Materials 132, 109638 (2023)

^dformally corresponds to the fundamental gap



Pure diamond electronic structures (densities of states)

Single-particle picture: DFT-predicted electronic structure of NV⁻ defect in bulk diamond



N, C except
3-fold coordinated C (C[3c])
C next to N (C[nN])

Gap states from under-coordinated C atoms: C[3c]

Defect orbital transition: $a_1 \rightarrow e$

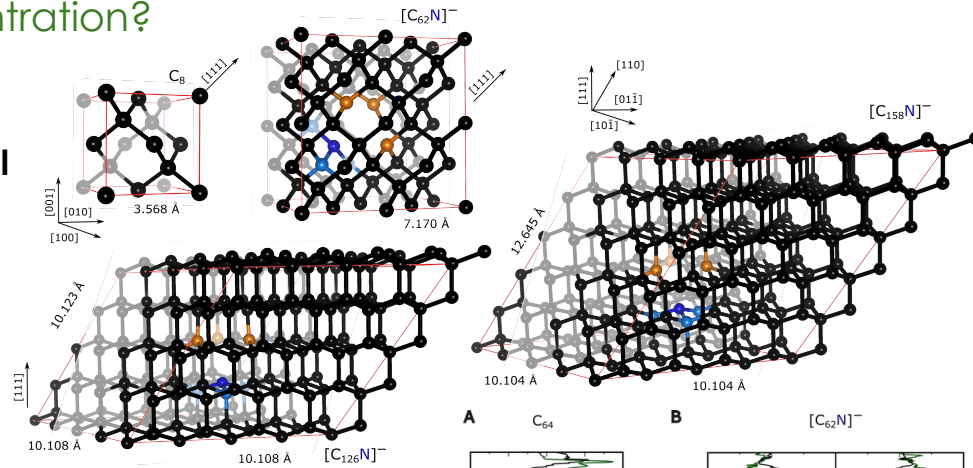
“Defect gap” (2.38 eV) higher than experimental optical vertical excitation (2.18 eV) and emission (1.95 eV)

Davies, G., Hamer, M. F. & Price, W. C. *Proceedings of the Royal Society of London. A. Mathematical and Physical Sciences* 348, 285 (1976)
Ma, Y., Rohlfing, M. & Gali, A. *Phys. Rev. B* 81, 041204 (2010)

Martirez, *arXiv*, 2505.01250 (2025)

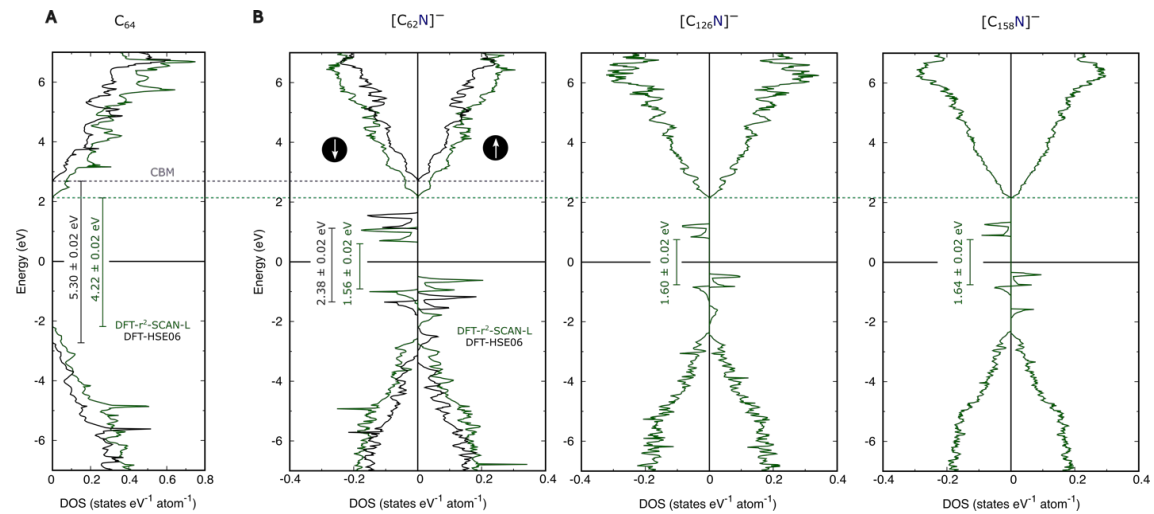
Are the defect states sensitive to defect concentration?

Supercell sizes



Yes, to some extent, defect “gap” a function of supercell size (~ 0.1 eV)

Electronic structure (densities of states)



pure

w/ NV⁻ defect

Excited-state Property Predictions via Capped Density Functional Embedding Theory

2. Optimize an embedding potential

$$W = E_{DFT}^{cl+cap1}[\rho^{cl}, V_{emb}] + E_{DFT}^{env+cap2}[\rho^{env}, V_{emb}] - \int V_{emb} (\rho^{full} + \rho^{cap1+cap2}) dr$$

$$\frac{\delta W}{\delta V_{emb}(\mathbf{r})} = \rho^{cl+cap1}(\mathbf{r}) + \rho^{env+cap2}(\mathbf{r}) - (\rho^{full} + \rho^{cap1+cap2}) \rightarrow 0$$

$$\rho^{cl+cap1}(\mathbf{r}) + \rho^{env+cap2}(\mathbf{r}) - \rho^{cap1+cap2} = \rho^{full}$$

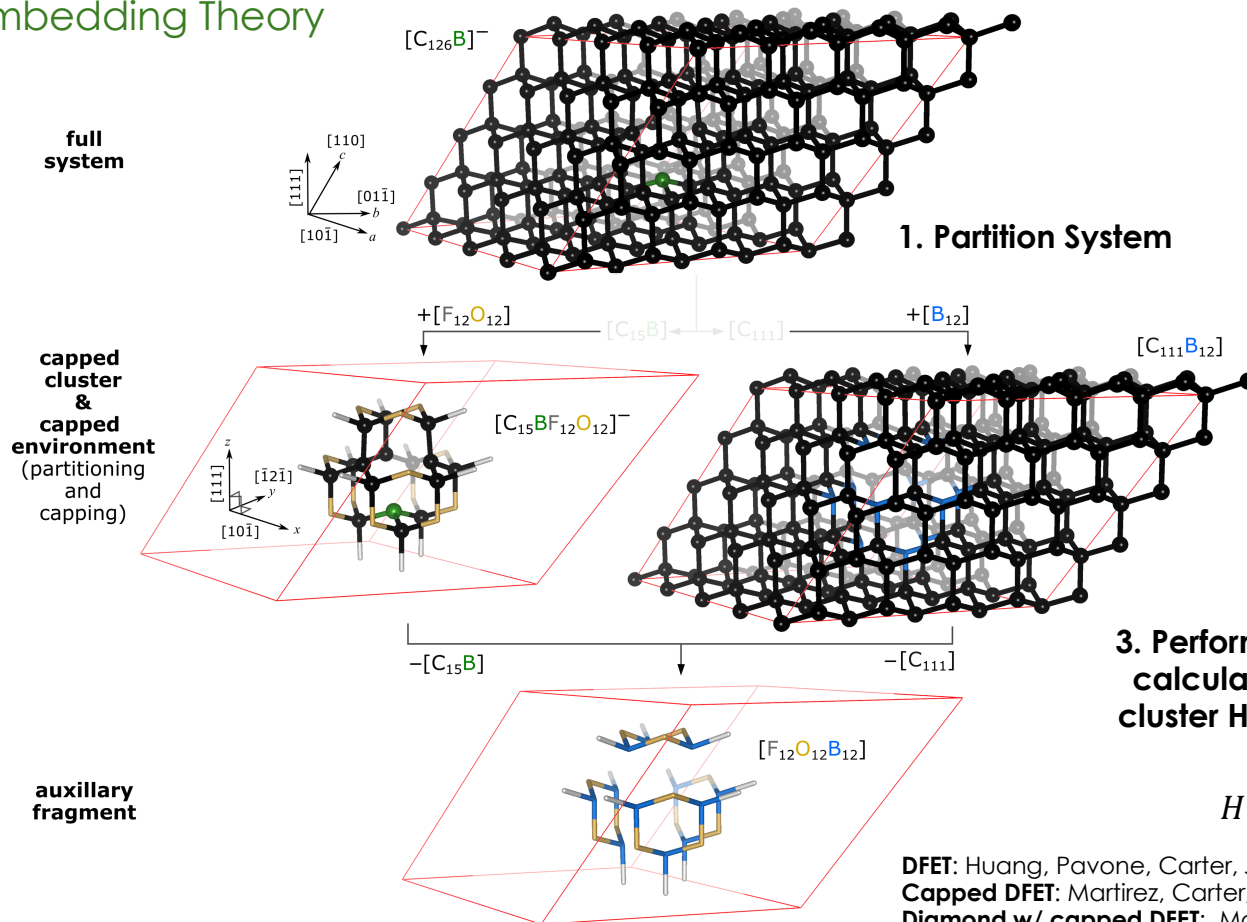
3. Perform correlated wavefunction theory calculations with modified non-periodic cluster Hamiltonian (no slowly convergent Coulomb interactions)

$$H = H^o + V_{emb} \quad \leftarrow \text{free of defect-defect interaction}$$

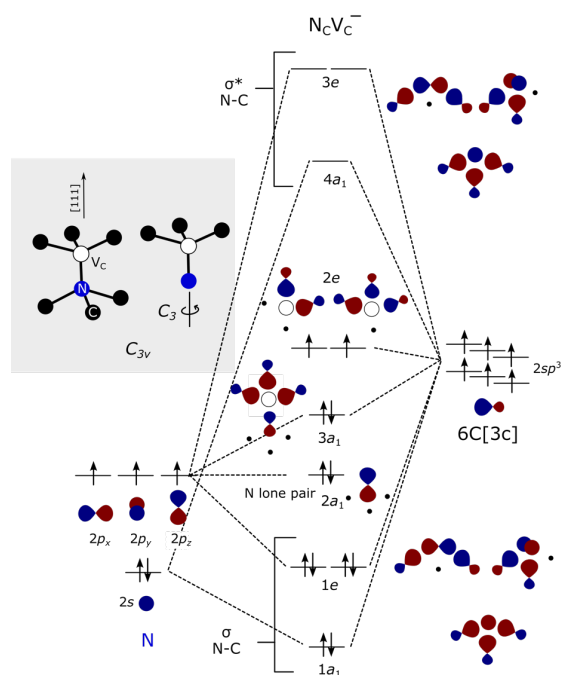
DFET: Huang, Pavone, Carter, J. Chem. Phys. 134, 154110 (2011)

Capped DFET: Martirez, Carter, J. Chem. Theory. Comput. 17, 4105 (2021)

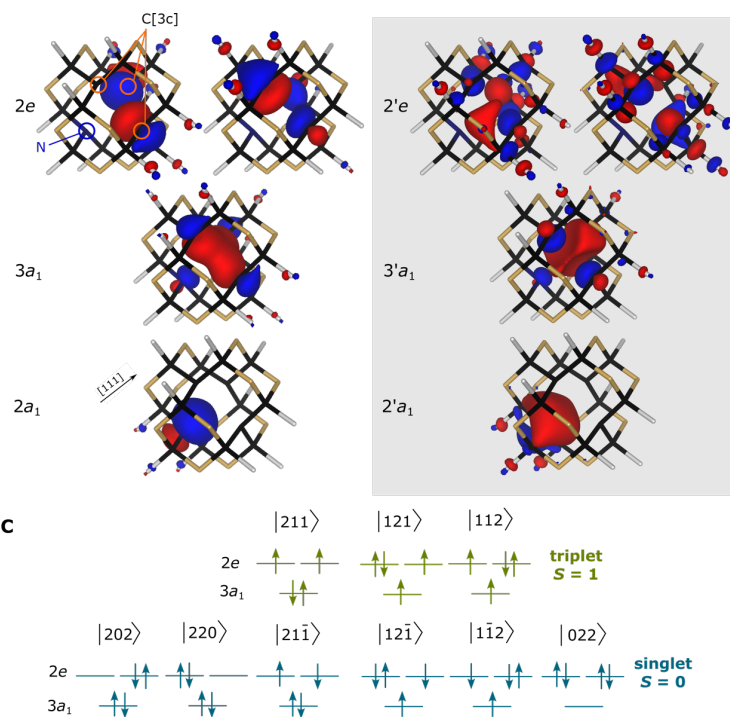
Diamond w/ capped DFET: Martirez, arXiv, 2505.01250 (2025)



Molecular orbital picture & multiconfigurational picture



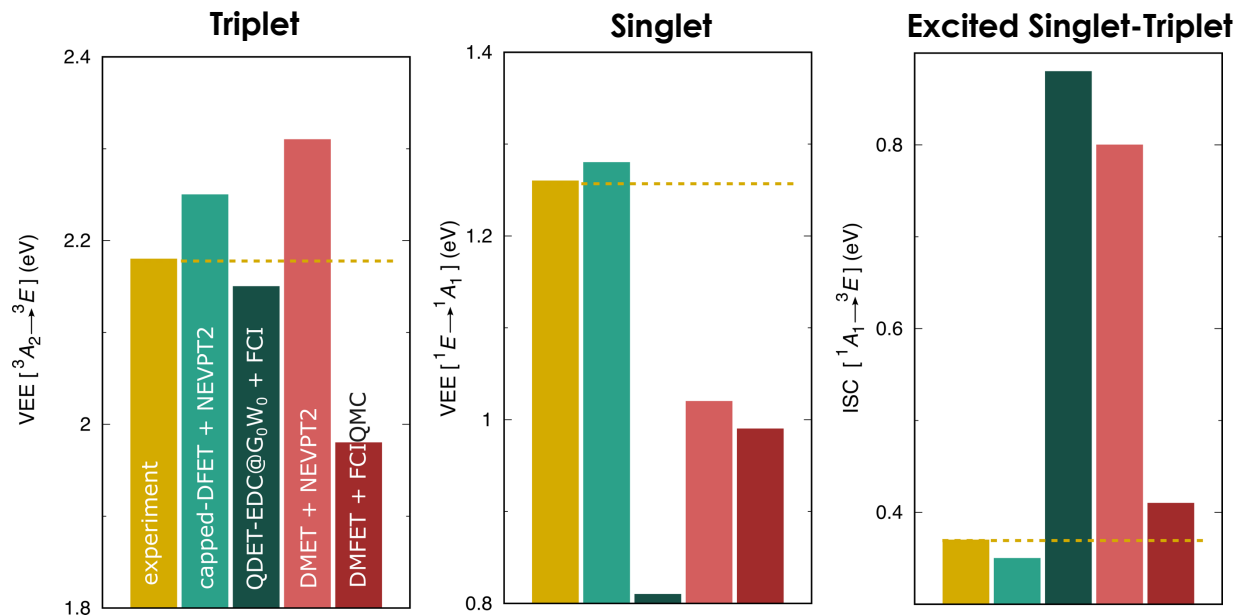
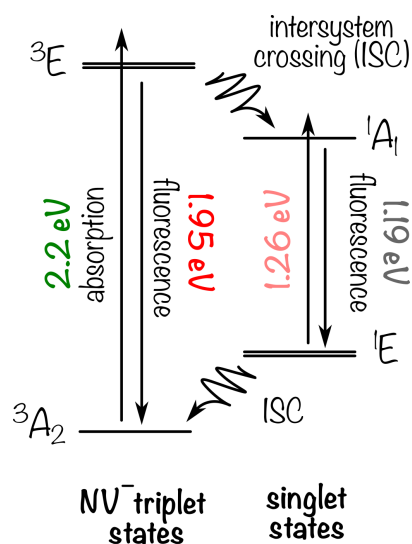
Point Group Symmetry + Molecular Orbital Diagram (explains spin structure and frontier orbital character) – **molecule-like not atom-like**



Calculated Natural Orbitals from multiconfigurational CW (verifies frontier orbital character and approximate symmetry)

Relevant electronic configurations (illustrates multiconfigurational nature of states)

Vertical Excitation Energy (VEE) Benchmark



Structures : **DFT-r2-SCAN-L**

Optimized embedding potential : **DFT-HSE06**

Excitation energies : **multistate CASSCF + NEVPT2**

Calculated properties:

Excitation energies, transition dipole moments → relative absorption strength and natural lifetimes, spin-orbit coupling → zero-field splitting

Martinez, *arXiv*, 2505.01250 (2025)

EXP: G. Davies et al., *Proc. R. Soc. Lond.* 348, 285 (1976); P. Kehayias, et al. *Phys. Rev. B*, 88, 165202 (2013); M. Goldman, et al. *Phys. Rev. B*, 96, 039905 (2017)

capped DFET + NEVPT2: embedded C₁₅NF₁₂O₁₂; Martinez, *arXiv* (2025)

QDET + FCI: C₅₁₀N; N. Sheng ... G. Galli, *JCTC*, 18, 3512 (2022)

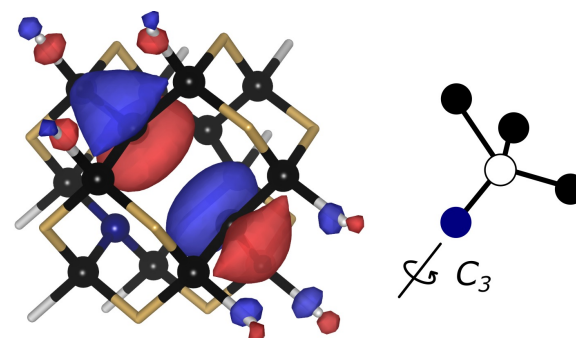
DMET + NEVPT2: C₂₁₄N; S. Haldar ... L. Gagliardi, *J. Phys. Chem. Lett.*, 14, 4273 (2023)

DMFET + FCIQMC: C₄₂H₄₂N; Y. Chen ... J. Chen, *Phys. Rev. B*, 108, 045111 (2023)

Method is accurate and rivals best-in-class!
Performs well across the board

Summary

- **Detailed benchmarking of the capped-DFET method** using embedded NEVPT2 using the negatively charged “**NV center**” in **diamond** as example
- We found **capped-DFET with emb-NEVPT2** reproduces VEEs and the ISC energy for spin triplet and singlet $N_C V_C^-$ with **errors less than 0.1 eV, rivaling more expensive methods**
- **Confirm** and thus **establish an accuracy-retaining method** that will potentially **enable fully ab initio QM characterization** of an array of **localized defects in diamond** that may be **key materials as building blocks for quantum devices**



Acknowledgements



U.S. DEPARTMENT
of **ENERGY**



Alkane dehydrogenation on Pt: U.S. Department of Energy, Office of Science Energy Earthshot Initiative as part of the **Non-equilibrium Energy Transfer for Efficient Reactions (NEETER)** under contract # **DE-AC05-00OR22725**



Methane activation on Cu: AFOSR MURI FA9550-15-1-0022

Quantum Diamond: Laboratory Directed Research and Development (LDRD) program under prime Contract No. DE-AC02-09CH11466